

Fukui Indices from Perturbed Kohn–Sham Orbitals and Regional Softness from Mayer Atomic Valences

T. Mineva,^{†,*} V. Parvanov,[†] I. Petrov,[†] N. Neshev,[†] and N. Russo^{‡,*}

Dipartimento di Chimica, Università della Calabria, I-87030 Arcavacata di Rende (CS), Italy and
Institute of Catalysis, Bulgarian Academy of Sciences, 1113 Sofia, Bulgaria

Received: September 23, 2000; In Final Form: December 19, 2000

Chemical reactivity descriptors are computed by the use of three alternative approaches derived within the framework of density functional theory. These schemes consider the computation of orbital Fukui indices, where all valence orbitals are taken into account; the Fukui indices of each atom in the molecule from the atomic resolved hardness matrix; and the atom in molecule softnesses, expressed in mixed LCAO representation of second quantization as functions of Mayer atomic valences. The hardness matrix is constructed from the Kohn–Sham orbitals by the use of the fractional occupation number concept and Janak’s extension of density functional theory. The site reactivity of molecules involved in radical attack reactions of some substituted olefins and isocyanide addition to dipolarophiles is rationalized in terms of the orbital and atomic resolved reactivity indices. The reactivity descriptors of thiophene, furane, and pyrrole are also reported and discussed. In addition, the nucleophilic attack on the allyl coordinated to the electronically asymmetric [Pd(phosphine)-(imine)] fragment was considered.

1. Introduction

The process of assigning of numbers to the chemical reactivity descriptors, such as global and local hardness, softness, and Fukui functions (FF) has greatly benefited from the development of density functional theory (DFT) based methods. The concept of hardness and softness was originally introduced by Pearson¹ to give insight into the nature of chemical reactivity. These concepts have proven useful in many ways but, without DFT tools, they were insufficient to make definite statements and were labeled by Pearson² as an example of “fuzzy logic”. Only when they were given a rigorous foundation within the framework of Density Functional Theory (DFT)³ by Parr and co-worker⁴ did it become possible to assign numerical values to these properties.

The chemical reactivity descriptors are identified in DFT as various energy derivatives with respect to the electron density.⁵ In this context, the hardness is defined as the second-order energy derivative, and the chemical potential is obtained as a first-order energy derivative. The softness is the inverse of the hardness. Although the chemical potential is a global characteristic of a quantum system, the hardness and softness are functions of position and characterize the local response at a given point inside the molecular region. These quantities in their local version were derived by Parr and Yang.⁵ Local properties are highly desirable in establishing a reactivity-oriented description of the molecules because the electron density distribution is the basis for understanding chemical reactivity. Moreover, concerning chemical reactivity, an important aspect is how the charge fluctuations in chemical systems affect, and are related to, the observed reactivity trends. A theoretical justification of the relationship between the electron charge fluctuations in atoms in a molecule and the chemical reactivity can be given within the hard and soft acids and bases (HSAB) principle of

Pearson.^{1,2} The relationship between reactivity and softness postulated in HSAB is rationalized in terms of local response properties of the system. On the other hand, the local hardness for a system in a global equilibrium state may be arbitrarily set equal to the global hardness, η , and can be taken to be an averaged of orbital contributions.⁶ Therefore, it is difficult to gain local information about the system from electronegativity and hardness.^{6,7}

The formalism of DFT allows one to introduce another important local variable, the Fukui function $f(r)$, originally defined by Parr and Yang⁵ as the first derivative of the chemical potential μ with respect to the external potential $v(r)$, or equivalently, as the first derivative of the electron density $\rho(r)$ with respect to the number of electrons N

$$f(\mathbf{r}) = \left[\frac{\delta\mu}{\delta v(\mathbf{r})} \right]_N = \left[\frac{\partial\rho(\mathbf{r})}{\partial N} \right]_v \quad (1)$$

The Fukui function measures how sensitive a system’s chemical potential is to an external perturbation at a particular point. Actually, great attention is paid to the computation of FF values as indicators of reactivity, which may avoid the precise study of the energy hypersurface. For a molecular or atomic system, the above derivatives are discontinuous and difficult to evaluate. Hence, different operational definitions of FF are still being developed^{8–14} and applied.^{9–11,14–28} The most common definitions used are those proposed by Yang and Parr⁵

$$f^+(\mathbf{r}) = \left(\frac{\partial\rho(\mathbf{r})}{\partial N} \right)_{v(\mathbf{r})}^+, \text{ for nucleophilic attack} \quad (2)$$

$$f^-(\mathbf{r}) = \left(\frac{\partial\rho(\mathbf{r})}{\partial N} \right)_{v(\mathbf{r})}^-, \text{ for electrophilic attack} \quad (3)$$

$$f^0(\mathbf{r}) = \left(\frac{\partial\rho(\mathbf{r})}{\partial N} \right)_{v(\mathbf{r})}^0, \text{ for radical attack} \quad (4)$$

[†] Institute of Catalysis, Bulgarian Academy of Sciences.

[‡] Dipartimento di Chimica, Università della Calabria.

The numerical approximation of the above formulas uses the finite differences in the density

$$f^+(r) = \rho_{(N=N_0+1)}(r) - \rho_{(N=N_0)}(r) \quad (5)$$

$$f^-(r) = \rho_{(N=N_0)}(r) - \rho_{(N=N_0-1)}(r) \quad (6)$$

$$f^0(r) = \frac{1}{2}(f^+(r) + f^-(r)) \quad (7)$$

Different levels of sophistication can be used for such computations according to the SCF method employed for density calculation. The latter equations have been further approximated, assuming that the density difference is just equal to the density of the populated orbital through the ionization or electron attachment process,²⁹ going in this way to the frontier orbitals theory, introduced by Fukui³⁰ in 1952. In the past decade, this approximation has been extensively applied in various chemical reactivity studies. There is some evidence in the literature^{31,32} that the consideration of only the frontier orbitals results in a poor approximation, regardless of the accuracy of the SCF procedure. Yang and Mortier¹¹ have called those values obtained by approximated integration of the FF over the atomic regions in molecules “condensed FF”. The exploration of the condensed FF in the studies of different systems and electrophilic and nucleophilic attack has led to the conclusion that condensed FF is very sensitive to the population analysis methods²⁷ used for charge partitioning of the molecule. An exhaustive review of the numerical FF approximations and their applicability as chemical reactivity descriptors is given in the recent work of Chermette.³³ The problems related to the accuracy of the approximations involved in FF determination motivates us to consider all Kohn–Sham valence orbitals in the FF computational scheme. Moreover, the FFs are not the absolute criterion of the system stability (reactivity). The stability of a system is determined by the eigenvalues of the matrix whose elements are energy derivatives of second order (Hessian) with respect to the coordinates or to the occupation numbers. Equation 1 shows that FF is not a Hessian element. Thus, the relationship between FF and reactivity is indirect, through the hardness or softness kernel.⁵ Hence, to provide a more reliable study of the reactivity, the computation of all local and global chemical descriptors is obligatory.

In the present article, a computational scheme for FF from all valence orbitals, proposed recently by us¹⁴ is employed in the study of the reactivity descriptors of thiophene, furane, and pyrrole. Radical attack reactions on some substituted olefins and isocyanide addition to dipolarophiles are also rationalized in terms of reactivity indices, obtained using the aforementioned method. These examples are also used for testing the reliability and the applicability of the atomic FF, computed from the hardness matrix, whose diagonal elements are the total atomic hardness and the off-diagonal ones, which are calculated through an empirical formula. A simple procedure³⁴ for deriving the atom in molecule (AIM) softness using the Mayer bond order analysis is also employed in the chemical reactivity study of the above-mentioned systems. Atomic FF and AIM softness values are also used for studying regioselectivity of nucleophilic attack on a [Pd(allyl)(phosphine)(imine)] complex model.

2. Method

The concept of hardness (η) has found its mathematical identification in DFT as the second derivative of the total energy with respect to the number of electrons, N ^{35,36}

$$\eta = \left[\frac{\partial^2 E}{\partial N^2} \right]_{v(\mathbf{r})} \quad (8)$$

or, equivalently

$$\eta = \left[\frac{\partial \mu}{\partial N} \right]_{v(\mathbf{r})} \quad (9)$$

where the chemical potential, μ , is the first derivative of the total energy relative to the electron number. Derivatives are taken at constant external potential, $v(\mathbf{r})$. Softness is defined as the inverse of hardness

$$S = \frac{1}{\eta} \quad (10)$$

Because the hardness and the softness are functions of the position, in addition to the global definition of η and S , the local hardness³⁷ and local softness³⁸ have been introduced as follows

$$\eta(\mathbf{r}) = \frac{1}{N} \int \frac{\delta^2 F[\rho]}{\delta \rho(\mathbf{r}) \delta \rho(\mathbf{r}')} \rho(\mathbf{r}') d\mathbf{r}' \quad (11)$$

$$s(\mathbf{r}) = \left[\frac{\partial \rho(\mathbf{r})}{\partial \mu} \right]_{v(\mathbf{r})} = \frac{1}{\eta} \left[\frac{\partial \rho(\mathbf{r})}{\partial N} \right]_{v(\mathbf{r})} \quad (12)$$

where $F[\rho]$ is the Hohenberg and Kohn universal functional.³⁹ These expressions are obtained through the integration of the hardness and softness kernels

$$\eta(\mathbf{r}, \mathbf{r}') = \frac{\delta^2 F[\rho]}{\delta \rho(\mathbf{r}) \delta \rho(\mathbf{r}')} \quad (13)$$

$$s(\mathbf{r}, \mathbf{r}') = - \left[\frac{\partial \rho(\mathbf{r}')}{\partial u(\mathbf{r})} \right]_{v(\mathbf{r})} = - \frac{1}{\eta} \left[\frac{\partial \rho(\mathbf{r}')}{\partial u(\mathbf{r})} \right]_{v(\mathbf{r})} \quad (14)$$

where $u(\mathbf{r})$ is the modified potential⁵

$$u(\mathbf{r}) = v(\mathbf{r}) - \mu = - \frac{\delta F[\rho]}{\delta \rho(\mathbf{r})} \quad (15)$$

The local hardness and local softness are reciprocals in the sense

$$\int s(\mathbf{r}) \eta(\mathbf{r}) d_2 = 1 \quad (16)$$

Other definition of local hardness have been proposed, but do not concern us here.

The detailed description of the theoretical approach employed in the present paper is given elsewhere.^{14,34} For easier reading of the work, we will sketch the main points of the methods.

2.1 Orbital Fukui Indices from Perturbed Kohn–Sham Orbitals. To compute local variables for a particular site in a molecule, one of the approaches proposed here is based on the fractional occupation number concept introduced into DFT by Janak⁴⁰ who generalized the earlier work of Slater⁴¹ using the X_α method. The computation of the orbital FF requires the values of the orbital hardness matrix elements, as demonstrated and discussed in detail by Mineva et al.¹⁴

In Janak's formulation of DFT, the KS one-electron orbital energies are defined as the first derivatives of the total energy with respect to the occupation numbers n_i

$$\epsilon_i = \left(\frac{\partial E}{\partial n_i} \right)_{i=1, \dots, N} \quad (17)$$

The study of a density change caused by external perturbations (i.e., the approach of a reagent to the system, the attachment of an electron, or an ionization process) is explored in DFT through Taylor's expansion of the total energy functional around the number of electrons N . Following Janak's extension of DFT for fractional occupations, the energy functional can be expanded around the state, characterized by the corresponding set of occupation numbers $(n_1^0, n_2^0, \dots, n_k^0)$ and by the corresponding KS-eigenvalues $\epsilon^0 = (\epsilon_1^0, \dots, \epsilon_k^0)$.

$$\begin{aligned} \Delta E &= \left(\frac{\partial E}{\partial N}\right)\Delta N + \frac{1}{2}\left(\frac{\partial^2 E}{\partial N^2}\right)(\Delta N)^2 + \dots = \\ &= \sum_i \frac{\partial E}{\partial n_i}\Delta n_i + \frac{1}{2}\sum_{ij} \frac{\partial^2 E}{\partial n_i \partial n_j}\Delta n_i \Delta n_j + \dots \end{aligned} \quad (18)$$

where $\Delta n_i = n_i - n_i^0$. The first derivatives with respect to the occupation numbers give the KS-eigenvalues (eq 17) and the second derivatives

$$\frac{\partial^2 E}{\partial n_i \partial n_j} = \eta_{ij} \quad (19)$$

give the hardness matrix as defined by Liu and Parr.⁴²

Because the KS-eigenvalues are defined through the Janak's theorem (eq 17) as first derivatives of the total DF-energy, the ij -th element of the hardness matrix can now be obtained as the first derivative of ϵ_i with respect to n_j ⁴³

$$\eta_{ij} = \frac{\partial \epsilon_i}{\partial n_j} \quad (20)$$

and to approximate them numerically using the finite difference formula

$$\eta_{ij} = \frac{\epsilon_i(n_j - \Delta n_j) - \epsilon_i(n_j)}{\Delta n_j} \quad (21)$$

The latter expression takes into account the response of the i -th orbital to the change of the occupation number of the j -th orbital, that is, the i -th orbital energy variation due to the j -th occupation number variation.

It is worth emphasizing that the use of Janak's extension of DFT in this reactivity index approach has two advantages: (1) the DF-energy functional can be expanded over the noninteger occupation numbers; and (2) in the calculation of hardness matrix elements, one takes only first-order derivatives (eq 20), thereby decreasing the numerical errors.

Because the local hardness and local softness are reciprocal to each other (eq 16), the softness matrix is the inverse of the hardness matrix

$$[s_{ij}] = [\eta_{ij}]^{-1} \quad (22)$$

Formula 22 holds for a nonsingular η_{ij} matrix. The total softness is obtained as an integral of the local softness⁵

$$S = \int s(\mathbf{r})d\mathbf{r} \quad (23)$$

Consequently, the total softness is an additive function of $s(\mathbf{r})$ and S can be approximated to

$$S = \sum_{ij} s_{ij} \quad (24)$$

Now the total hardness becomes

$$\eta = \frac{1}{S} = \frac{1}{\sum_{ij} s_{ij}} \quad (25)$$

Having obtained the hardness matrix according to eq 21, let us turn back to Taylor's expansion of the energy functional (eq 18). If the Taylor series is truncated at the second term (linear approximation), then the energy behavior around the equilibrium state, (ϵ_i^0, n_i^0) , can be studied topologically, not as a function of the position in real molecular space but instead as a function of the eigenvalues and occupation numbers. The search for the extreme of the energy functional $\Delta E(n, \epsilon)$ upon the density variation leads to a linear system of equation as follows

$$\frac{\partial \Delta E}{\partial n_i} = \epsilon_i + \sum_j \eta_{ij}\Delta n_j = 0 \quad i = 1 \dots N \quad (26)$$

The solution of eq 26 at a given ϵ_i and with $\text{Det}(\eta_{ij}) \neq 0$ with respect to Δn_i gives

$$\Delta n_i = -\sum_{j=1}^N [\eta_{ij}]^{-1}\epsilon_j = -\sum_{j=1}^N s_{ij}\epsilon_j \quad (27)$$

Considering the system with a fixed deviation of the occupation numbers from their equilibrium value, $\sum_i \Delta n_i = \Delta N$, the set of equations (26) becomes

$$\epsilon_i + \sum_{j=1}^N \eta_{ij}\Delta n_j + \lambda = 0 \quad i = 1, \dots, N$$

$$\sum_i \Delta n_i = \Delta N \quad (28)$$

In the last equation, λ is the Lagrange multiplier and can be interpreted as the effective electronegativity, or the negative of the chemical potential. Because the Kohn–Sham orbital energies can be understood as orbital electronegativity,⁴² by taking the derivative of λ relative to ϵ_i (eq 28) one obtain the approximation to the orbital FF.

$$f_i = \frac{\partial \lambda}{\partial \epsilon_i} = \frac{\partial n_i}{\partial N} \quad \sum_i f_i = 1 \quad (29)$$

The relation between the orbital Fukui indices and the orbital softness $s_i = \sum_j s_{ij}$, is

$$f_i = \left(\frac{\partial n_i}{\partial \mu}\right)\left(\frac{\partial \mu}{\partial N}\right) = \eta s_i \quad (30)$$

Equations 24–30 provide an operational scheme to compute orbital FF, in the vicinity of the system equilibrium point using occupation number representation within the Kohn–Sham DFT formalism.

2.2 Fukui Indices from Atomic Resolved Hardness Matrix.

Applying the Sanderson equalization principle,⁴⁴ the energy functional $\Delta E(n, \epsilon)$ (see eq 18) can be expanded over the density variation of the atoms in the molecule, instead of the density change of each orbitals. Hence, the η_{ii} elements in the hardness matrix are now constructed by the total hardness values of each of the atoms in the molecule. The off-diagonal elements are obtained from Ohno's⁴⁵ empirical formula

$$\eta_{AB} = \frac{1}{\sqrt{b_{AB}^2 + R_{AB}}}$$

$$b_{AB} = \frac{2}{2\eta_{AA} + 2\eta_{BB}}$$

where, R_{AB} is the distance between the atoms A and B in the molecule AB.

In this way, the atoms are allowed to “interact” with each other within the molecule.

2.3. AIM Softness from Mayer Atomic Valence. The expression for the AIM softness is also derived in the mixed LCAO representation of second quantization as simple functions of Mayer bond order indices and Mayer atomic valences.⁴⁶ The approach used here essentially deals with the concepts of electron localization and charge fluctuations. These quantities are connected with the hardness and softness, respectively,³⁵ the higher the electron localization, the larger the hardness, or, the higher the charge fluctuation the larger the softness. Fluctuation formulas for local softness and the softness kernels for grand-canonical ensemble at finite temperatures have also been derived by Harbola et al.⁶ The physical meaning of such fluctuation formulas and their possible applications in catalysis and charge-transfer processes is extensively described by these authors. Moreover, the ensemble descriptions make it possible to take softness and local softness as a mean value of the charge fluctuations and to take hardness and local hardness as a mean value of the orbital energy fluctuations.

The regional softness fluctuation formulas, in the present work, are obtained using the partitioning in MO-LCAO space, as an alternative to atoms in molecules partitioning in real space^{47–49} and following the earlier ideas of Bader et al.⁵⁰

Let us consider some (arbitrary for the moment) subdomain Ω of a molecule, a general estimate of the degree of electron localization in this subdomain is given by the magnitude of the relative electron charge fluctuation $\lambda(\Omega)$ ⁵⁰

$$\lambda(\Omega) = \frac{1}{N(\Omega)} \langle \tilde{N}(\Omega) \tilde{N}(\Omega) \rangle - N(\Omega)^2 \quad (31)$$

where the averaging $\langle \dots \rangle$ is with respect to the molecular ground state, and $N(\Omega)$ is the average electron occupancy in Ω (can be noninteger)

$$N(\Omega) = \int_{\Omega} \rho(r) dr \quad (32)$$

The larger the relative fluctuation $\lambda(\Omega)$ within some subregion, Ω , the smaller is the degree of electron localization in this subregion, and vice versa.

Note that eq 31 is analogous to eq 2.9 in ref 6, where the averaging is within the grand-canonical ensemble formalism.

The regional electron number operator $\tilde{N}(\Omega)$ entering eq 31 can be conveniently expressed in second quantization as

$$\tilde{N}(\Omega) = \sum_{\sigma} \int_{\Omega} \hat{n}_{\sigma}(r) dr \equiv \sum_{\sigma} \int_{\Omega} \hat{\psi}_{\sigma}^{\dagger}(r) \hat{\psi}_{\sigma}(r) \quad (33)$$

where σ is the spin index and \hat{n}_{σ} is the electron-density operator expressed as a product of the Heisenberg (fermionic) field operators, obeying the standard fermionic anti-commutation relations⁵¹

$$\{\hat{\psi}_{\sigma_1}^{\dagger}(r_1) \hat{\psi}_{\sigma_2}(r_2) + \hat{\psi}_{\sigma_2}(r_2) \hat{\psi}_{\sigma_1}^{\dagger}(r_1)\} = \delta_{\sigma_1 \sigma_2} \delta(r_1 - r_2) \quad (34)$$

In the second quantization, the observable electron density

$$\rho_{\sigma} = \langle \hat{n}_{\sigma} \rangle = \langle \hat{\psi}_{\sigma}^{\dagger} \hat{\psi}_{\sigma} \rangle$$

plays the role of a physical field associated with the Heisenberg field operators. Using the fermionic anti-commutation relations (eq 34) and the idempotency property of the electron-density operator (due to the Pauli exclusion principle)⁵¹

$$\hat{n}_{\sigma}^2 = \hat{n}_{\sigma}; \langle \hat{n}_{\sigma}^2 \rangle = \langle \hat{n}_{\sigma} \rangle = \rho_{\sigma} \quad (35)$$

one can re-express eq 31 in terms of the density–density correlator kernel $S_{\sigma_1 \sigma_2}(1,2)$

$$\lambda(\Omega) = \frac{1}{N(\Omega)} \sum_{\sigma_1, \sigma_2} \int_{\Omega} dr_1 \int_{\Omega} dr_2 S_{\sigma_1 \sigma_2}(r_1, r_2) \quad (36)$$

with

$$S_{\sigma_1 \sigma_2}(1,2) = \langle \hat{n}_{\sigma_1}(1) \hat{n}_{\sigma_2}(2) \rangle - \rho_{\sigma_1}(1) \rho_{\sigma_2}(2) \quad (37)$$

The correlator kernel contains important information about the many electron system. For example, the potential part of the KS DFT exchange–correlation energy can be expressed in terms of local charge fluctuations^{52,53} as

$$\tilde{E}_{xc}[\rho_1, \rho_2] = \frac{1}{2} \sum_{\sigma_1, \sigma_2} \int_{\infty}^3 dr_1 \int_{\infty}^3 dr_2 \frac{1}{|r_1 - r_2|} \left\{ S_{\sigma_1 \sigma_2}(r_1, r_2) - \frac{1}{2} n(r_1) \delta(r_1 - r_2) \right\} \quad (38)$$

Various other properties of a chemical system are also closely related to the magnitude of the electron charge fluctuations in different subregions. Let us, for instance, divide the molecular space into non-overlapping subregions attached to each of the bound atoms A, B, C, ... (following the topological partitioning scheme of Bader⁵⁰ for example)

$$\Omega_{\text{mol}} \equiv \Omega_A \cup \Omega_B \cup \dots$$

If one specifies the region Ω as one of the AIM subdomains, then one obtains the relative charge fluctuation within this AIM region. It can be described equivalently also in terms of intra-atomic charge–charge correlators C_{AA} reflecting the magnitude of the total charge fluctuation in Ω_A

$$C_{AA} \equiv \lambda(\Omega_A) \cdot N(\Omega_A) = \sum_{\sigma_1, \sigma_2} \int_{\Omega_A} dr_1 \int_{\Omega_A} dr_2 S_{\sigma_1 \sigma_2}(r_1, r_2) \quad (39)$$

Similarly, one can define interatomic charge–charge correlators describing charge fluctuations between two different AIM regions

$$C_{AB} = \sum_{\sigma_1, \sigma_2} \int_{\Omega_A} dr_1 \int_{\Omega_B} dr_2 S_{\sigma_1 \sigma_2}(r_1, r_2) \quad (40)$$

Using the mixed LCAO expansion of the density and density operator in the second quantization (eq 35) and neglecting the three-center regional integrals, after some algebra, one obtains mixed LCAO expressions of charge–charge correlators

$$C_{AA} \approx \langle \hat{q}_A \hat{q}_A \rangle - q_A^2 \quad (41)$$

$$C_{AB} \approx \langle \hat{q}_A \hat{q}_B \rangle - q_A q_B \quad (42)$$

where \hat{q}_A, q_A are the (hermitized) atomic-charge operators of Mayer and its average value, respectively.

Following such an approach, the popular Mulliken formula appears as a particular case of the more general Mayer formula^{46,47} when the ground-state averaging is performed at SCF single determinant level

$$C_{AA}(\text{SCF}) = q_A(\text{Mull}) - \sum_{\sigma} \sum_{a_1, a_2 \in A} (P^{\sigma} \cdot S)_{Aa_1, Aa_2} (P^{\sigma} \cdot S)_{Aa_2, Aa_1} \quad (43)$$

where the summation runs over all possible combinations of the orbital indices $a_1, a_2 \in A$, S is the overlap matrix, and P^{σ} is the conventional bond-order matrix.

KS SCF formulas for the interatomic charge–charge correlators are derived

$$C_{AB}(\text{SCF}) = - \sum_{\sigma} \sum_{a \in A} \sum_{b \in B} (P^{\sigma} \cdot S)_{Aa, Bb} (P^{\sigma} \cdot S)_{Bb, Aa}, A \neq B \quad (44)$$

The above expression is directly related to the bond-order index (P_{AB}) introduced by Mayer as a genuine SCF MO-LCAO descriptor of chemical bonds^{46,47}

$$P_{AB} = -2C_{AB}(\text{SCF}) \quad (45)$$

The interatomic correlators are negatively defined and reflect a bonding attraction between two atoms (at least for covalent bonding). However, one should bear in mind that the SCF approximation usually tends to overestimate the magnitude of the charge fluctuations in the bonding region, that is, to exaggerate the covalent component of the bonding. As in the case of the atomic charges, only the exchange contribution to the charge–charge correlators is included at KS SCF level, as long as the KS determinant is the reference wave function in resolving the ground-state averages. This is in sharp contrast to the situation with the KS DFT ground-state energy. The latter is calculated as a functional of the electron density in an exact manner, (without referring to wave functions) and includes electron correlation through the XC part of the functional. However, the presence of the exchange–correlation term in the KS SCF potential and the condition that the KS electron density is equal to the exact density have a subtle influence on the considered one-electron and two-electron averages, even when they are resolved at KS SCF level. How to go beyond this level in calculating ground-state averages other than the energy is not a trivial matter in KS DFT because correlated wave functions are not the focus of this method. One possibility for proceeding in this direction is to use recent advances in KS DFT perturbation theory.^{54,55}

Using these idempotency properties together with eqs 43 and 44, the following relation between the intra-atomic and the interatomic correlators is readily obtained at SCF level

$$C_{AA}(\text{SCF}) = - \sum_B C_{AB}(\text{SCF}), B \neq A \quad (46)$$

It also reveals another nontrivial chemical meaning of the charge–charge correlators: the term on the right-hand side of eq 45 is directly related to the AIM LCAO valence (V_A), as defined and discussed in refs 46–48

$$V_A = 2C_{AA}(\text{SCF}) = -2 \sum_B C_{AB}(\text{SCF}) \quad (47)$$

In other words, the larger the charge fluctuations in a given

AIM region, the more extensively this AIM is involved in bonds with other AIMs. As can be shown³⁴ the values of the so defined AIM valence are often close to those expected from the classical valence picture.

These procedures were also recently successfully employed for orbital hardness and AIM softness computations for studying hydrogen-bonded 1,2-Dihydroxybenzene.⁵⁶

2.4 Computaional Details. For the present computation of the reactivity indices, the DFT based code deMon⁵⁷ was used. All the atoms constituting the studied species were described by basis sets of double- ζ quality⁵⁸ and gradient-corrected functionals of Perdew⁵⁹ for correlation and Perdew and Wang⁶⁰ for exchange energies were employed. The calculations of the hardness matrix elements and, consequently, the total hardness and FF values, were carried out by taking into account the occupied valence orbitals together with the LUMO. The variations of the occupation numbers Δn_i were set to be 0.5 for all the studied molecules except for the selected dipolarophiles for which $\Delta n_i = 0.005$ is used.

The atomic total hardness, necessary for atomic FF calculations, were obtained from the orbital resolved hardness matrix and eq 25. The η values equal to 9.496, 6.339, 9.959, 4.871, and 8.571 eV for H, C, N, O, and F, respectively, were taken from ref 12, and $\eta = 3.828, 7.923, 5.524, 8.272,$ and 3.891 eV for Si, P, S, Cl, and Pd, respectively, were computed for the present study.

3. Results and Discussion

We have chosen to treat three different applications that are of great importance in organic chemistry for studying both the reaction mechanism and the regioselectivity. The considered examples are reactivity and selectivity of pyrrole, furane, and thiophene, radical attack to the substituted olefins and 1,3-cycloaddition of HNC to some selected dipolarophiles. In addition, we have considered a transition metal containing system. We have deliberately studied systems, for which previous theoretical data for reactivity descriptors, computed mainly by the use of a HOMO–LUMO or IP-AE approximations, exist.^{25,26,61}

Reactivity Trends and Selectivity of Some Five-Member Conjugated Systems. Let us briefly summarize the theoretical literature on this subject. The reactivity behavior of pyrrole, furane, and thiophene toward an electrophilic attack has been the subject of different theoretical investigations.^{62–65} Electrostatic potential and charge distribution studies^{62,63} favor the β -substitutions, whereas condensed FF indices values from the semiempirical hardness matrix in atomic resolution⁶⁴ and those from relaxed Kohn–Sham orbital¹⁵ correctly predict the electrophilic attack to the α -carbon.

Our results are collected in Table 1. The systems under consideration are characterized by different degrees of lone-pair participation in the π -electron sextet of the ring. Because the total hardness measures the degree of electron localization, or, equivalently, the molecular polarizability and resonance energy, the η value from all the employed methods correctly describes the lone pair localization order of the heteroatoms. In particular, oxygen in furane has the most localized lone-pair (highest η value), confirming that furane can exhibit olefin properties, whereas the other 2 heterocycles behave rather like benzene. As shown in Table 1, all levels of the employed approximations indicate that the hardest species is furane followed by pyrrole and thiophene.

Concerning an electrophilic attack (i.e., H^+), reactivity descriptor values in Table 1 give information on the various

TABLE 1: Reactivity Descriptors (Total Hardness, η , in eV; Fukui Indices, f and AIM Softness, s) for Pyrrole, Furane and Thiophene

descriptors	pyrrole	furane	thiophene
η^a	6.321	6.625	6.064
f_H^a	0.663	0.855	0.819
f_L^a	0.545	0.336	0.181
η^b	6.354	6.573	5.970
f_H^b	0.345	0.434	0.846
f_L^b	0.180	0.055	0.051
f_{H-1}^b	0.680	0.567	0.076
f_{H-2}^b	0.250	-0.480	0.410
η^c	7.776	7.946	7.380
$f_{C\alpha}^c$	0.153	0.141	0.185
$f_{C\beta}^c$	0.121	0.122	0.100
f_X^c	-0.038	0.086	0.281
$s_{C\alpha}^d$	3.896	3.882	3.858
$s_{C\beta}^d$	3.980	3.950	3.998
s_X^d	2.942	2.480	2.486

^a From HOMO–LUMO difference. ^b From orbital resolved hardness matrix. ^c From atomic resolved hardness matrix. ^d From Mayer atomic valences.

aspects of the reaction mechanism. According to the HSAB principle, the species with the hardest HOMO, that is, with the lowest f_H value, will be the most active toward H^+ approach because H^+ is a hard electrophile. FF from orbital resolved hardness matrix correctly suggest that the less active species is thiophene having the highest FF value for HOMO. f_H of pyrrole (0.345) and furane (0.434) are similar and almost half of that for thiophene ($f_H = 0.846$), which means that these two species are more active toward H^+ approach. This trend accounts for the known behavior of these five-member heterocycles. On the contrary, the f_H values obtained by the use of simple HOMO–LUMO difference show an order, which does not correlate with the expected chemical behavior. In general, this approximation is quite rough because, even for HOMO (or LUMO) controlled reactions, all valence electrons take part in the processes and in any case would be of crucial importance for a correct numerical evaluation of the reactivity descriptors.^{14,24,28}

As previously mentioned, there are no doubts that the electrophilic substitutions on the aromatic rings prefer the C_α -position.⁶⁶ To study the selectivity trend, the Fukui indices from the atomic resolved hardness matrix, as well as the local softness from the Mayer atomic valences, were computed and collected in Table 1. These values distinguish the C_α atoms as the more reactive center in all cases because C_α Fukui indices have the highest values. Our FFs, obtained from an atomic resolved hardness matrix, show a trend similar to those previously found from the condensed FF values by Michalak et al.¹⁵ The same message can be extracted from the AIM softness. The less bonded atom is characterized by a lower value of the AIM softness. From Table 1, it can be seen that the values of the AIM softnesses reveal also C_α for all species to be the preferred site in substitution reactions.

Regioselectivity of Free Radical Addition to the Substituted Olefins. Because of the importance of the free radical addition to olefins in many fields of modern chemistry, numerous studies with conventional molecular orbital computations have been devoted to this subject, with the aim of rationalizing the addition mechanism, including the regioselectivity. The potential energy surfaces for a series of radical addition to olefins are available in the literature.^{67–69} Recently, Chandra and Nguyen²⁶ have used the condensed Fukui function in attempt to apply this reactivity descriptor approach for prediction of the preferred attack site in addition reactions of

TABLE 2: Reactivity Indices of Substituted Olefins^a

molecule	atom	f_i	s_i
$H_2C=CHF$	C^1	0.232	3.882
	C^2	0.213	4.002
$H_2C=CHNH_2$	C^1	0.207	3.898
	C^2	0.179	3.984
$H_2C=CHOH$	C^1	0.212	3.880
	C^2	0.173	4.062
$H_2C=CHCN$	C^1	0.199	3.906
	C^2	0.143	3.920
$H_2C=CHCHO$	C^1	0.186	3.878
	C^2	0.124	3.856
$HFC=CF_2$	C^1	0.196	4.122
	C^2	0.178	3.944
$HFC=CHCl$	C^1	0.194	3.964
	C^2	0.198	3.860

^a Fukui indices, f_i , from the atomic resolved hardness matrix, and AIM softness, s_i , from Mayer atomic valences. C^1 represents the carbon atom at the less-substituted end.

TABLE 3: Reactivity Indices from the Orbital Resolved Hardness Matrix of Substituted Olefins^a

molecule	η	orbital	ϵ_i	MO coefficients	f_i
$H_2C=CHF$	7.942	H-1	-10.1258	F (11 Px), F (14 Pz)	0.390
		H	-8.9408	C^1 (50 Py), C^2 (32 Py)	0.686
		L	-6.5905	C^1 (46 Py), C^2 (47 Py)	0.119
$H_2C=CHNH_2$	7.021	H-1	-8.0618	C^2 (31 Py), N (43 Py)	0.172
		H	-4.9732	C^1 (46 Py), N (32 Py)	0.875
		L	-0.5434	C^1 (46 Py), C^2 (44 Py)	0.446
$H_2C=CHOH$	7.160	H-1	-8.9601	O (38 Px), O (14 Pz)	0.018
		H	-5.6898	C^1 (50 Py), O (27 Py)	1.484
		L	-0.5434	C^1 (42 Py), C^2 (48 Py)	0.494
$H_2C=CHCN$	6.653	H-1	-8.3705	C^1 (47 Py), C^2 (25 Py)	0.411
		H	-7.3181	C^3 (29 Py), N (39 Py)	0.580
		L	-2.9284	C^3 (46 Py), N (26 Py)	0.058
$H_2C=CHCHO$	6.810	H-1	-7.4740	C^1 (43 Py), C^2 (36 Py)	0.600
		H	-6.0366	O (16 Px), O (57 Pz)	0.094
		L	-3.1335	C^1 (37 Py), C^3 (26 Py)	0.037
$HFC=CF_2$	8.030	H-1	-9.6695	F ¹ (57 Pz), F ¹ (14 Py)	-0.700
		H	-6.5350	C^1 (39 Py), C^2 (28 Py)	0.363
		L	-1.0248	C^1 (43 Py), C^2 (44 Py)	0.193
$HFC=CHCl$	6.900	H-1	-7.9823	C^1 (73 Pz)	0.698
		H	-6.3984	C^1 (28 Py), C^2 (32 Py)	2.396
		L	-1.5091	C^1 (41 Py), C^2 (49 Py)	-0.290

^a Total hardness, η , and orbital energies, ϵ_i , are in eV. C^1 represents the carbon atom at the less substituted end.

two radicals (CH_3 and CF_3) to a series of olefins. We consider it of interest to make a comparison between the reactivity descriptor values from different working approaches. For this reason, we have treated a series of previously studied olefins ($CH_2=CHX$, $X=F, NH_2, OH, CN, COH, Cl$).²⁶ Our values are given in Tables 2 and 3 and Figure 1. Because the total hardness can be related to the barrier height for the same types of reactions, it is interesting to verify if the η -trend of the considered olefins correlates with the known barrier height values in the case of CH_3 reactions.⁶⁷ As shown in Figure 1 and Table 2, the η values from both the orbital and atomic resolved hardness matrix decrease correctly with the decrease in corresponding barrier height.

Fukui indices from atomic resolved hardness matrix and AIM softness in Table 2 indicate that radical addition prefers the less substituted carbon (C^1) end in agreement with the Markovnikov rule and previous studies.⁶⁷ Exceptions occur for $HFC=CF_2$ and $HFC=CHCl$. For these systems, it is worth noting that, experimentally, CH_3 radical add to the more substituted carbon atom (C^2), whereas CF_3 show a reverse preference.^{67–69} The reported atomic FF in Table 2 for C^1 and C^2 of $HFC=CHCl$ are almost equal, and thus, both the carbon atoms are expected to be equally reactive toward radical attack. In the case of $HFC=$

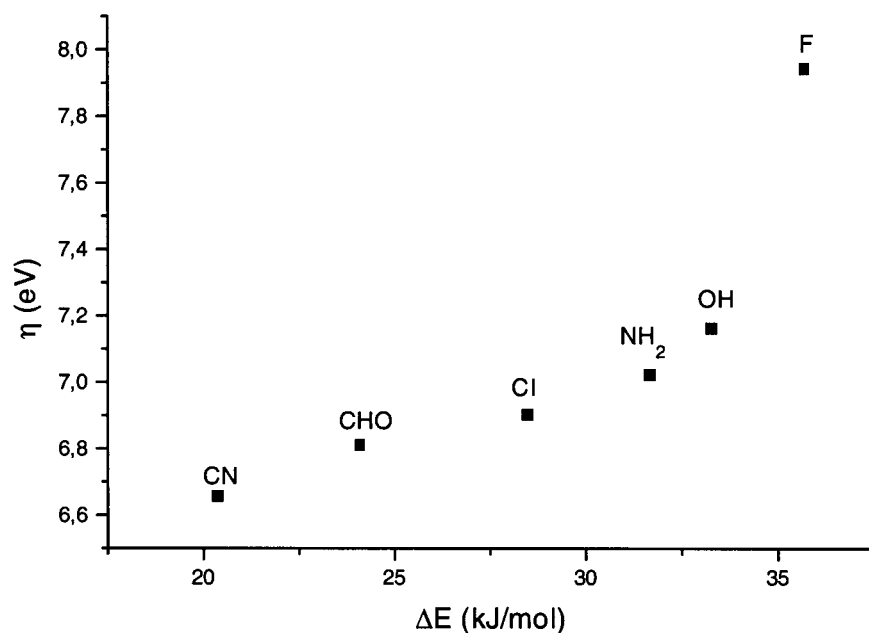


Figure 1. Total hardness, η , from orbital hardness matrix versus energy barrier height, ΔE , for CH_3 addition to olefins ($\text{CH}_2=\text{CHX}$, $\text{X}=\text{F}$, NH_2 , OH , CN , COH , Cl). ΔE values are taken from ref 65.

CF_2 , the less substituted carbon is found to be more reactive, that is, $f_i(\text{C}^1) > f_i(\text{C}^2)$. From the AIM softness values in Table 2, one concludes that for these two olefins the less bonded atom is C^2 ($s_{\text{C}^2} < s_{\text{C}^1}$), and therefore, C^2 would be the preferred site for the radical addition.

As previously noted,²⁶ the calculated properties refer to the isolated fragments and the electronic rearrangements during the reactions are not considered.

To gain a better insight into radical addition to these olefins, we have calculated the FF from the orbital resolved hardness matrix. Table 3 contains f_i for HOMO and LUMO orbitals as well as for HOMO-1. The LUMO of all the olefins treated show a lower f_i value with respect to the HOMO. The main character of the former is essentially the same for all the systems (the main orbital coefficients are those of C^1 and C^2), with the exception of $\text{H}_2\text{C}=\text{CHCN}$ and $\text{H}_2\text{C}=\text{CHCHO}$, where the nitrogen and C^3 atoms, respectively, participate in the formation of LUMO. We underline that these two olefins act as weak donors in the CH_3 radical attack.⁶⁷ The composition of the HOMO orbital reveals that in the case of $\text{H}_2\text{C}=\text{CHF}$, $\text{H}_2\text{C}=\text{CHNH}_2$, $\text{H}_2\text{C}=\text{CHOH}$, $\text{HFC}=\text{CHCl}$, and $\text{HFC}=\text{CF}_2$ the C^1 character dominates. Because the CH_3 and CF_3 radicals are soft radicals,² the orbitals governing the reaction would be those with higher FF values (softer orbitals). The FFs in Table 3 indicate that the HOMO is the most reactive orbital for these five species and because the HOMO is constructed predominantly from C_1 coefficients, the less substituted atom is the preferred center. Therefore, the relationship between the atomic reactivity indices and the orbital resolved is coherent. For the other two species, the correlation is not immediate if the HOMO-1 orbital is not be considered. Here, this orbital becomes significant because it is formed predominantly by the C^1 atom. Looking at the HOMO and LUMO Fukui index values (Table 3), in the cases of $\text{H}_2\text{C}=\text{CHCN}$ and $\text{H}_2\text{C}=\text{CHCHO}$, one notes that the f_i values are close to zero, whereas for HOMO-1 they are $f_i = 0.411$ for $\text{H}_2\text{C}=\text{CHCN}$ and $f_i = 0.600$ for $\text{H}_2\text{C}=\text{CHCHO}$. Thus, the studied reaction for these two olefins is HOMO-1 controlled. This information cannot be obtained correctly from the condensed Fukui indices, where only HOMO and LUMO influences are taken into account.

Isocyanide Addition to Dipolarophiles. The importance of cycloaddition reactions in organic chemistry is well-known. The isocyanide molecule has been found to act as a nucleophile in the [2+1] cycloaddition reactions of a series of heteronuclear dipolarophiles containing double bonds such as the $\text{R}_2\text{C}=\text{X}$ ($\text{X}=\text{SiH}_2$, PH , NH , O , or S) systems.⁶¹ Accurate theoretical studies that deal with the potential energy surfaces for the reaction of HNC with $\text{R}_2\text{C}=\text{X}$ ($\text{X}=\text{SiH}_2$, PH , NH , O , S) are available in the literature.⁷⁰ In addition, works devoted to the application of DFT-based descriptors on these and similar isocyanide cycloadditions^{61,71} have recently appeared. In all of these studies, the reactivity indices were determined through the finite difference between the vertical electron affinity and ionization potential and the charge difference between the neutral and the charged species.

It was pointed out that the reaction paths are not simple because HNC approaches the dipolarophiles indirectly, in two elementary steps: first, H^+ from the isocyanide dissociation interacts with the X group and then the CN^- moiety attaches the dipolarophile. Furthermore, previous ab initio studies have shown that the formation of two different transition states that lead to the same products can be viewed as an asynchronism in the formation of new bonds, one bond being formed earlier than the other.⁷⁰

Our reactivity indices are collected in Tables 4 and 5. The computed energy barrier heights⁷⁰ decrease in the order $\text{NH} > \text{O} > \text{PH} > \text{S} > \text{SiH}_2$, whereas our η decrease as $\text{O} > \text{NH} > \text{S} > \text{PH} > \text{SiH}_2$. For completeness, we report the behavior of hardness derived from the softness previously computed by Chandra et al.,⁶¹ $\text{NH} > \text{O} > \text{PH} > \text{SiH}_2 > \text{S}$. A funny puzzle emerges. As mentioned before, these reactions have more than one reaction channel, and the comparison was made with the lowest transition state energy. Furthermore, as pointed out recently by Gazquez,³⁶ the activation energy is proportional to the difference in hardness between the transition state and the reactant, so further computations are necessary in order to well characterize the correlation between hardness and barrier heights in this kind of reaction.

In the considered reactions, the isocyanide acts as a nucleophile system, being the electron donor, in agreement with

TABLE 4: Reactivity Indices of Considered Dipolarophiles^a

molecule	atom	f_i	s_i
HN≡C	C	0.576	2.622
H ₂ C=SiH ₂	Si*	0.815	3.892
	C	0.108	3.822
H ₂ C=PH	P	0.224	2.878
	C*	0.299	3.814
H ₂ C=NH	N	0.088	3.062
	C*	0.358	3.986
H ₂ C=O	O	0.063	2.244
	C*	0.164	3.970
H ₂ C=S	S	0.106	2.042
	C*	0.493	3.860

^a Fukui indices, f_i , from atomic resolved hardness matrix, and AIM softness, s_i , from Mayer atomic valences. The preferred site of attack is shown by*, indicated on the basis of ab initio calculations from ref 68.

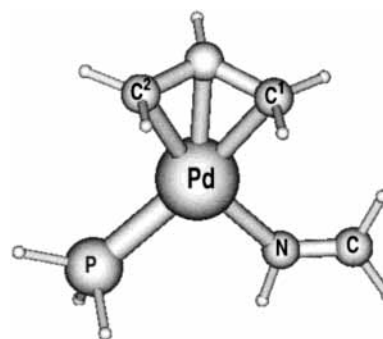
TABLE 5: Reactivity Indices from Orbital Resolved Hardness Matrix of Considered Dipolarophiles^a

molecule	η	orbital	ϵ_i	main MO coefficients	f_i
HN≡C	8.52	H	-7.6637	C(52 S), C(40 Pz)	0.422
H ₂ C=SiH ₂	5.58	H	-5.7023	C(57 Py), Si(41 Py)	2.399
		L	-2.2160	C(36 Py), Si(60 Py)	0.201
H ₂ C=PH	6.63	H	-6.8101	C(51 Py), P(48 Py)	0.758
		L	-2.8730	C(45 Py), P(52 Py)	0.516
H ₂ C=NH	8.35	H	-6.4158	N(58 Pz), N(14 S)	0.209
		L	-1.8960	C(56 Py), N(40 Py)	0.356
H ₂ C=O	9.31	H	-6.3222	O(34 Px), O(37 Pz)	0.498
		L	-2.8175	C(64 Py), O(33 Py)	0.663
H ₂ C=S	7.99	H	-5.5912	S(47 Px), S(42 Pz)	-0.070
		L	-3.7727	C(54 Py), S(34 Py)	0.750

^a Total hardness, η , and orbital energies, ϵ_i , are in eV.

previous indications.⁶⁷⁻⁷⁰ So, the atom with the larger Fukui index in the dipolarophile will govern the regioselectivity. Table 4 shows that our f_i 's account well for the preferred attack site for all the compounds considered. Similar indications come from the regional softness analysis (see s_i in Table 4). For example, in CH₂=PH, the s_i values are 3.814 and 2.878 for the carbon and phosphorus atoms, respectively. This means that the C is far from its formal valence (4) than P (3). Analogously, in H₂C=O, H₂C=S, and H₂C=NH, the X heteroatoms are over-bonded, and carbon appears to be the preferred site for the reaction process. The only exception is H₂C=SiH₂, for which our s_i 's predict the carbon to be more reactive in disagreement with the previous ab initio computations.⁷⁰ A comparison between our regional descriptors and the previous ones reveals that condensed Fukui functions even when computed using the electrostatic potential driven charges fail to predict correctly the regioselectivity for HNC addition to H₂C=PH and H₂C=S dipolarophiles.

Finally, the analysis of Table 5, in which the orbital Fukui indices are given together with the orbital compositions, reveals that the f_i of the HOMO is higher than that of the corresponding one for the LUMO only in the cases of the H₂C=SiH₂ and H₂C=PH systems. So, for these two species, they are unable to explain the preferred site because, for the nucleophilic attack, the reactions occurs preferentially with the orbital that presents the higher f_i value (generally the LUMO). These failures may be due to the fact that the hardness matrix elements are close to each other, and therefore, the corresponding determinant is close to zero. For this reason, the hardness matrix elements were obtained perturbing each valence Khon-Sham orbital with 0.005 electrons. These systems would be good examples for testing the influence of third derivatives of the energy with

**Figure 2.** Model of Pd(allyl)(phosphine)(imine) complex, considered for atomic and AIM softness calculations of the catalyst precursor.**TABLE 6: AIM Softness, s_i , and Fukui Indices from Atomic Resolved Hardness Matrix, f_i for Pd(allyl)(phosphine)(imine)**

descriptors	C	C _{trans-N}	C _{trans-P}
s_i	1.951	1.941	1.934
f_i	0.044	0.053	0.055

respect to the occupation number, the third term in the Taylor expansion,¹⁴ on the reactivity descriptors.

Regioselectivity of Nucleophilic Attack on [Pd(allyl)-(phosphine)(imine)] Model. We conclude by discussing the AIM softnesses and FF from the atomic resolved hardness matrix of a transition metal containing system. [Pd(allyl)-(phosphine)(imine)] complexes, containing either C₂-symmetric or electronically asymmetric bidentate chiral ligands, are widely explored in palladium-catalyzed functionalization of allyl substrates.⁷²⁻⁷⁴ For a symmetrical 1,3-disubstituted allyl coordinated in an η^3 -mode, attack at C¹ and C³ (see Figure 2) yields the opposite enantiomers.⁷⁵ Therefore, the site of nucleophilic attack determines the chirality of the product, and thus, the catalytically active complex shows a single reactive geometry. For these reasons, the determination of the site of nucleophilic attack has attracted the attention of experimentalists,⁷⁶ as well as of theoreticians.^{77,78} The carbon atoms C¹ and C³ are distinguished via the different donor atoms in trans positions as C_{trans-P} and C_{trans-N}, respectively.

We have calculated the reactivity indices of a simplified model of the catalyst precursor. The phosphine donor was modeled by PH₃, and the pyrazole was modeled by an imine HN=CH₂ (Figure 2). The same model is used by Gilardoni et al.²⁵ to rationalize the regioselectivity in terms of condensed Fukui functions. For our calculations, the geometry parameters are taken from ref 76. The AIM softness values in Table 6 reveals that the C_{trans-P} is the less bonded carbon atom and, therefore, the most reactive. The same conclusion can also be drawn from the atomic FF, reported in Table 6. From these calculations C_{trans-P} is characterized by the largest FF value, which is an indication that it would be the center participating predominantly in the nucleophilic reaction. The condensed Fukui functions previously computed²⁵ also predict the C_{trans-P} carbon to be more electrophilic than C_{trans-N}. These results are in agreement to the experimental⁷⁶ and theoretical^{76,77} evidence that a nucleophilic attack on coordinated allyls occurs at C_{trans-P}. However, under reaction conditions, the rotation of the allyl averages both sites with respect to the electronic asymmetry.⁷⁵ It is worth noting that our reactivity indices lead to the conclusion that the C_{trans-P} center would be the most reactive, but they show only a slight difference between C_{trans-P} and C_{trans-N} centers. The central carbon atom is well distinguished via the highest AIM softness and the lowest atomic FF not to be a possible center in a nucleophilic reaction. So, from our

reactivity indices (Table 6) we can certainly confirm previous calculations on related systems,⁷⁸ which reveal that the reaction is frontier controlled rather than charge controlled because the latter would yield a nucleophilic attack on the central carbon.

Conclusions

In this work, we have presented three alternative approaches to obtain DFT- chemical descriptors. The applications show that they can give insight into different reaction mechanisms. The atomic FF and AIM softness values can be useful in rationalizing the regioselectivity and direction effects, whereas the indicators in orbital resolution are needed to explain reactivity effects. The atomic FF are relative easy to obtain, and therefore, they can be used as reasonable indicators for large systems, for which full orbital analysis becomes too time-consuming.

Although the chemical descriptors can be considered individually as promising tools, giving a qualitative indication and explanation of chemical phenomena, consideration of more than one indicator would lead to more reliable conclusions. In any case, their validity will be further tested, and the theoretical development of the methodology is necessary.

Acknowledgment. Financial support from University of Calabria and MURST (Progetto Nazionale Sistemi a Grande Interfase) is greatly appreciated.

References and Notes

- Pearson, R. G. *J. Am. Chem. Soc.* **1963**, *85*, 3533.
- Pearson, R. G. *Chemical Hardness*; Wiley-VCH: Weinheim, 1997.
- Kohn, W.; Sham, L. *Phys. Rev.* **1965**, *140*, A1133.
- Parr, R. G.; Donnelly, R. A.; Levy, M.; Palke, W. E. *J. Chem. Phys.* **1978**, *69*, 4491.
- Parr, R. G.; Yang, W. *Density Functional Theory of Atoms and Molecules*; Oxford University Press: New York, 1989.
- Harbola, M. K.; Chattaraj, P. K.; Parr, R. G. *Israel J. Chem.* **1991**, *31*, 395.
- Ayers, P. W.; Parr, R. G. *J. Am. Chem. Soc.* **2000**, *122*, 2010.
- Nalewajski, R. F.; Korchowiec, J. *Charge Sensitivity Approach to Electronic Structure and Chemical Reactivity*; World-Scientific: Singapore, 1997.
- Cohen, M. H. In *Topics in Current Chemistry Vol 183: Density Functional Theory IV—Theory of Chemical Reactivity*; Nalewajski, R. F., Ed.; Springer-Verlag: Heidelberg, 1986; p 143.
- Korchowiec, J.; Gerwens, H.; Jug, K. *Chem. Phys. Lett.* **1994**, *222*, 58.
- Yang, W.; Mortier, W. J. *J. Am. Chem. Soc.* **1986**, *108*, 5708.
- Senet, P. *J. Chem. Phys.* **1996**, *105*, 6471; **1997**, *107*, 2516.
- Liu, G. H. *J. Chem. Phys.* **1997**, *106*, 165.
- Mineva, T.; Neshev, N.; Russo, N.; Sicilia, E.; Toscano, M. *Adv. Quantum Chem.* **1999**, *33*, 273.
- Michalak, A.; De Proft, F.; Geerlings, P.; Nalewajski, R. F. *J. Phys. Chem. A* **1999**, *103*, 762.
- Gazquez, J. L.; Vela, A.; Galwan, M. In *Structure and Bonding, Electronegativity*; Sen, K., Ed.; Springer-Verlag: Heidelberg, 1987; Vol. 66, p 79.
- Komorowski, L.; Lipinski, J. *Chem. Phys.* **1991**, *157*, 45.
- Cioslowski, J.; Mixon, S. T. *J. Am. Chem. Soc.* **1991**, *113*, 4142.
- Chattaraj, P. K.; Cedillo, A.; Parr, R. G. *J. Chem. Phys.* **1995**, *103*, 7645.
- De Proft, F.; Liu, S.; Geerlings, P.; Parr, R. G. *Pol. J. Chem.* **1998**, *72*, 1737.
- Balewander, R.; Komorowski, L. *J. Chem. Phys.* **1998**, *109*, 5203.
- Geerlings, P.; De Proft, F.; Martin, J. M. L. In *Recent Developments in Density Functional Theory*; Seminario, J., Ed.; Elsevier: Amsterdam, 1996; p 773.
- Nalewajski, R. F. *Phys. Chem. Chem. Phys.* **1991**, *1*, 1037.
- Mineva, T.; Russo, N.; Sicilia, E.; Toscano, M. *Theor. Chem. Accounts* **1999**, *101*, 388.
- Gilardoni, F.; Weber, J.; Chermette, H.; Ward, T. R. *J. Phys. Chem. A* **1998**, *102*, 3607.
- Chandra, A. K.; Nguyen, M. T. *J. Chem. Soc., Perkin Trans. 2* **1997**.
- Roy, R. K.; Pal, S.; Hirao, K. *J. Chem. Phys.* **1999**, *110*, 8236.
- Marino, T.; Russo, N.; Sicilia, E.; Toscano, M.; Mineva, T. *Adv. Quantum Chem.* **2000**, *36*, 93.
- Langenaeker, W.; De Decker, M.; Geerlings, P.; Rayemaekers, P. *J. Mol. Struct. (THEOCHEM)* **1990**, *207*, 115.
- Fukui, K.; Yonezawa, Y.; Shingu, H. *J. Chem. Phys.* **1952**, *20*, 722.
- Langenaeker, W.; Demel, K.; Geerlings, P. *J. Mol. Struct. (THEOCHEM)* **1991**, *234*, 329.
- Langenaeker, W.; Demel, K.; Geerlings, P. *J. Mol. Struct. (THEOCHEM)* **1992**, *259*, 317.
- Chermette, H. *J. Comput. Chem.* **1999**, *20*, 129–154.
- Neshev, N.; Proynov, E.; Mineva, T. *Bul. Chem. Comm.* **1998**, *30*, 482.
- Parr, R. G.; Pearson, R. G. *J. Am. Chem. Soc.* **1983**, *105*, 1512.
- Gazquez, J. L. *Struct. Bonding* **1993**, *80*, 27.
- Berkowitz, M.; Parr, R. G. *J. Chem. Phys.* **1998**, *88*, 2554.
- Yang, W.; Parr, R. G. *Proc. Natl. Acad. Sci. U.S.A.* **1985**, *82*, 6723.
- Hoehenberg, P.; Kohn, W. *Phys. Rev. B* **1964**, *136*, 864.
- Janak, J. F. *Phys. Rev. B* **1978**, *18*, 7165.
- Slater, J. C. *The Self-Consistent Field for Molecules and Solids*; McGraw-Hill: New York, 1974; Vol. 4.
- Liu, G. H.; Parr, R. G. *J. Am. Chem. Soc.* **1995**, *117*, 3179.
- Neshev, N.; Mineva, T. In *Metal–Ligand Interactions: Structure and Reactivity*; Russo, N., Salahub, D. R., Eds.; Kluwer: Dordrecht, 1996; p 361.
- Sanderson, R. T. *Chemical Bonds and Bond Energy*, 2nd ed.; Academic: New York, 1976.
- Ohno, K. *Adv. Quantum Chem.* **1967**, *3*, 39.
- Mayer, I. *Chem. Phys. Lett.* **1983**, *97*, 270. Mayer, I. *Chem. Phys. Lett.* **1985**, *117*, 396.
- Mayer, I. *Int. J. Quantum Chem.* **1983**, *23*, 391. Mayer, I. *Theor. Chim. Acta (Berlin)* **1985**, *67*, 315.
- De Giamgiagi, M. S.; Giambiagi, M.; Jorge, E. E. *Theor. Chim. Acta* **1985**, *68*, 337.
- Pitanga, P.; Giambiagi, M.; de Giamgiagi, M. S. *Chem. Phys. Lett.* **1986**, *128*, 411.
- Bader, R. F. W. *Atoms in Molecules: A Quantum Theory*; Oxford University Press: Oxford, 1990.
- Raimes, S. *Many-Electron Theory*; North-Holland: Amsterdam-London, 1972.
- Langreth, D. C.; Perdew, J. P. *Phys. Rev. B* **1977**, *15*, 2884.
- Anderson, Y.; Langreth, D. C.; Lundquist, B. I. *Phys. Rev. Lett.* **1996**, *76*, 102.
- Gorling, A.; Levy, M. *Phys. Rev. A* **1994**, *50*, 196.
- Gonze, X. *Phys. Rev. A* **1995**, *52*, 1096.
- Vedernikova, I.; Proynov, E.; Salahub, D.; Haemers, A. *Int. J. Quantum Chem.* **2000**, *77*, 161.
- St-Amant, A. Ph.D. Thesis, Universite de Montreal, Canada 1992.
- Godbout, N.; Salahub, D. R.; Andzelm, J.; Wimmer, E. *Can. J. Chem.* **1992**, *70*, 560.
- Perdew, J. P. *Phys. Rev. B* **1986**, *33*, 8822.
- Perdew, J. P.; Wang, Y. *Phys. Rev. B* **1986**, *33*, 8800.
- Chandra, A. K.; Geerlings, P.; Nguyen, M. T. *J. Org. Chem.* **1997**, *62*, 6417.
- Politzer, P.; Weinstein, H. *Tetrahedron* **1975**, *31*, 915.
- Nalewajski, R. F.; Koninski, M. *J. Mol. Struct.: THEOCHEM* **1988**, *165*, 365.
- Nalewajski, R. F.; Korchowiec, J. *Acta Phys. Pol.* **1989**, *A76*, 747.
- Bacskay, G. B.; Martoprawiro, M.; Mackie, J. C. *Chem. Phys. Lett.* **1999**, *300*, 321, and references therein.
- Beilstein Handbook of Organic Chemistry*; Reiner Luckenbach, Ed.; Springer-Verlag: Berlin, 1988; Vol.10.
- Wong, M. W.; Pross, A.; Radom, L. *J. Am. Chem. Soc.* **1993**, *115*, 11 050.
- Tedder, J. M.; Walton, J. C. *Adv. Phys. Org. Chem.* **1978**, *16*, 1.
- Poblet, J. M.; Canadell, E.; Sordo, T. *Can. J. Chem.* **1983**, *61*, 2068.
- Nguyen, M. T.; Van Keer, A.; Vanquickenborne, L. G. *Chem. Ber.* **1997**, *130*, 69.
- Nguyen, L. T.; Le T. N.; De Proft, F.; Chandra, A. K.; Langenaeker, W.; Nguyen, M. T.; Geerlings, P. *J. Am. Chem. Soc.* **1999**, *121*, 5992.
- Consiglio, G.; Waymouth, R. M. *Chem Rev.* **1989**, *89*, 257.
- Godleski, S. A. In *Comprehensive Organic Synthesis*; Trost, B.; Fleming, I., Eds.; Pergamon: Oxford, Vol. 4, 1991; p.585.
- Hayashi, T. In *Catalytic Asymmetric Synthesis*; Ojima, I., Ed.; VCH: New York, 1993; p 325.
- Ward, T. R. *Organometallics* **1996**, *15*, 2836.
- Togni, A.; Burckhardt, U.; Gramlich, V.; Pregosin, P. S.; Salzman, R. *J. Am. Chem. Soc.* **1996**, *118*, 1031.
- Bloch, P. E.; Togni, A. *Organometallics* **1996**, *15*, 4125.
- Curtis, M. D.; Einstein, O. *Organometallics* **1984**, *3*, 887.